

01.1;08.3;09.4

Lasing in Tamm plasmon-based microcavities with intracavity metallic contacts and organic active area

© K.M. Morozov¹, A.V. Belonovski^{1,2}, E.I. Girshova^{1,2}, V.V. Nikolaev²

¹ ITMO University, St. Petersburg, Russia

² Alferov Federal State Budgetary Institution of Higher Education and Science Saint Petersburg National Research Academic University of the Russian Academy of Sciences, St. Petersburg, Russia
E-mail: morzconst@gmail.com

Received December 10, 2021

Revised January 13, 2022

Accepted January 13, 2022

Vertical-cavity surface-emitting laser design with organic light-emitting material 4,4'-bis[4-(di-*p*-tolylamino)styryl]biphenyl and intracavity metal contacts of two types are proposed. In the first design, two Bragg mirrors and two thin metal layers adjacent to the active region utilizes. In the second design one Bragg mirror with a thin metal layer and for the second mirror the thick metal layers uses. Mode structure, the spatial distribution of the optical fields, Purcell factor and the dependence of the output power on the pump power were calculated.

Keywords: Tamm plasmon, organic semiconductor, vertical-cavity surface-emitting laser, exciton.

DOI: 10.21883/TPL.2022.04.53161.19104

Vertical-cavity surface-emitting lasers (VCSELs) [1,2] are used widely in various branches of science and technology. One of the factors limiting their efficiency is the problem of electrical pumping of the active region. A possible solution to this problem is the use of semiconductor [3] or metallic [4] intracavity contacts. Considerable progress has been made in the study of VCSELs with an organic active region in recent years [5,6].

In the present study, two types of microcavities with intracavity metallic contacts and an organic light-emitting DPAVBi (4,4'-bis[4-(di-*p*-tolylamino)styryl]biphenyl) [7] material serving as an active region are compared.

Let us consider two types of microcavities with intracavity contacts: a microcavity formed by two Bragg reflectors (BRs) (type I) and a microcavity with one BR and one thick metallic mirror (type II) (Fig. 1, *a*). A BR is comprised of five SiO₂ (81 nm)/Ta₂O₅ (55 nm) pairs. Owing to the presence of intracavity metallic layers, both types of cavities may provide electrical pumping of the organic layer [4]. The thickness of the intracavity silver layer is 40 nm, the thickness of the thick metallic mirror is 616 nm, and the thickness of the organic DPAVBi layer is 55 nm. The dynamics of photoluminescence (PL) decay of DPAVBi and the diagram of its molecule are presented in Fig. 1, *b*. Three localized optical modes are present in structure type I: two Tamm plasmon modes localized at the metal–BR interface and the Fabry–Pérot mode localized between two metal layers. Cavity type II is regarded as an alternative design of the structure with one BR substituted by a thick silver layer. Two optical modes (Tamm plasmon mode and Fabry–Pérot mode) interact in such a cavity. The dispersions of optical eigen states obtained by approximating the reflection spectra (calculated using the transfer matrix method) are presented

in Fig. 2 for both types of cavities. The results of calculation of the mode Purcell factor performed using the *S*-quantization method [8] are also shown in this figure. The microcavities were designed so that the DPAVBi PL peak is located at 2.6 eV, while the absorption peak of this material is at an energy of 3 eV. Thus, one mode in the considered cavities may generate radiation, and the other may provide efficient optical pumping.

The influence of the considered two types of microcavities on laser generation was analyzed using rate equations. It is assumed in the considered model that the optical pumping of structures is carried out through the BR by a laser emitting at 3 eV with an incidence angle of 60° (the regions enclosed in ovals in Fig. 2). The structures themselves, in turn, emit in the normal direction with an energy of 2.52 eV (type I) and 2.56 eV (type II). The dynamic behavior may be characterized by a system of equations [9] for the exciton density at the upper vibrational sublevel of the excited state (N_{exc}) and the lower energy vibrational sublevel (N_{gr}) and the photon density in the cavity mode (*S*):

$$\frac{dN_{exc}(t)}{dt} = A \frac{P_{pump}}{\hbar\omega_p} \frac{1}{V_p} - k_{rel}N_{exc}(t) - k_{nr}N_{exc}(t), \quad (1a)$$

$$\begin{aligned} \frac{dN_{gr}(t)}{dt} &= k_{rel}N_{exc}(t) - (F_p k_r + k_{nr})N_{gr}(t) \\ &\quad - \sigma_g v_{gr} S(t) N_{gr}(t), \end{aligned} \quad (1b)$$

$$\frac{dS(t)}{dt} = F_p \Gamma \beta k_r N_{gr}(t) + \Gamma \sigma_g v_{gr} S(t) N_{gr}(t) - k_{cav} S(t). \quad (1c)$$

The first term in Eq. (1a) characterizes optical pumping with power P_{pump} and energy $\hbar\omega_p = 3$ eV, where *A* is the absorption coefficient of the structure for an incidence angle

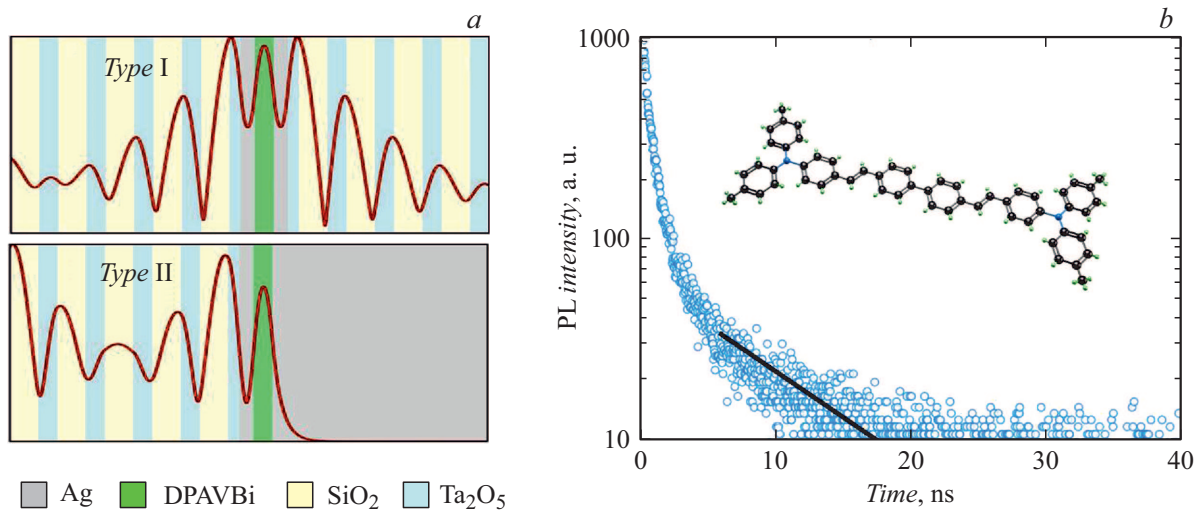


Figure 1. *a* — Diagram of microcavities with intrametallic layers. Solid curves represent the distributions of the electric field of the eigen mode of cavities type I (with an energy of 2.52 eV) and type II (with an energy of 2.56 eV) for a TE-polarized wave. *b* — Dynamics of photoluminescence decay of the DPAVBi layer with a thickness of 60 nm. The DPAVBi molecule structure is shown in the inset. A color version of the figure is provided in the online version of the paper.

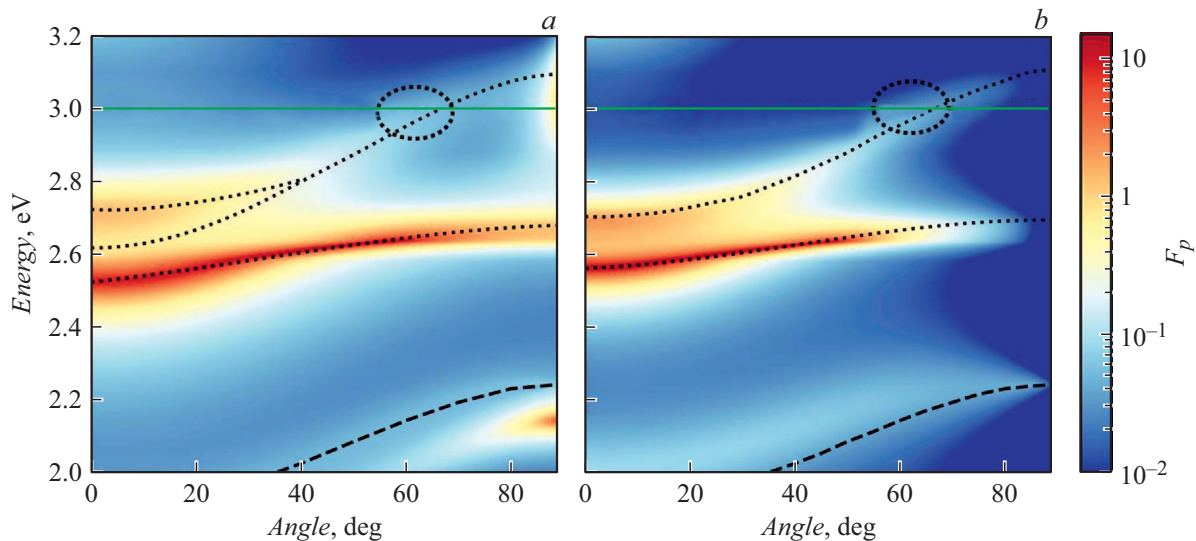


Figure 2. Distributions of mode Purcell factor F_p over energy and incidence angle for a microcavity with intrametallic layers (type I) (*a*) and a microcavity with an intrametallic layer and a metallic mirror (type II) (*b*) for the TE polarization and a dipole positioned in the middle of the DPAVBi layer. The dashed curve represents the dispersion of the BR edge state, and dotted curves correspond to the dispersions of cavity modes. The horizontal solid line denotes the position of the DPAVBi absorption peak. Ovals mark the regions of incidence angles and energies where the structures are pumped. A color version of the figure is provided in the online version of the paper.

of 60° and V_p is the volume of the structure region (set by thickness $d_{cav} = 55$ nm of the active region and radius $a_{las} = 25 \mu\text{m}$ of the excitation laser spot). The second and the third terms characterize the oscillatory relaxation of excitons to the low-energy excited state and the nonradiative loss with rates k_{rel} and k_{nr} , respectively. The relaxation rate in organic materials of this kind is on the order of 10^{15} s^{-1} . Radiative decay is neglected for this level, since the overwhelming majority of radiative transitions proceed from the lower energy vibrational sublevel.

Equation (1b) characterizes the dynamics of the density of excited states in the lower energy vibrational sublevel. The second term in it has the meaning of spontaneous radiative decay of an excited state with rate k_r , which is intensified by Purcell factor F_p , and nonradiative loss with rate k_{nr} (, which matches the corresponding value in Eq. (1a)). The third term is stimulated emission that is characterized by the following quantities: stimulated emission cross-section σ_g , which has a characteristic value of $4 \cdot 10^{-16} \text{ cm}^2$, and group velocity of light $v_{gr} = c/n$.

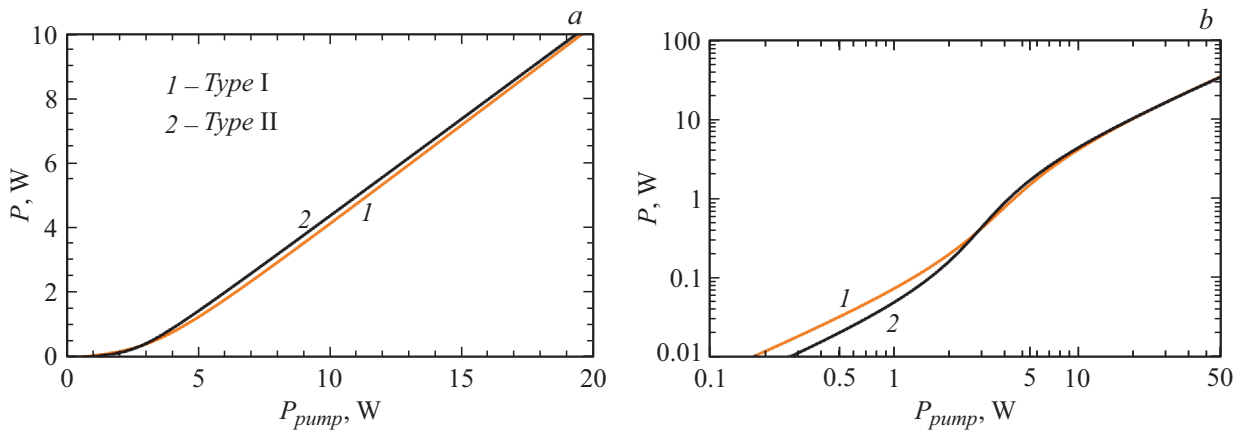


Figure 3. Dependences of the output power on the pumping power for two types of microcavities on linear (a) and log-log (b) scales.

The third equation corresponds to the photon density in the optical mode of the structure. The first two terms characterize the influx of photons due to spontaneous and stimulated emission, respectively. Parameter Γ is the optical limiting factor, β is the contribution of spontaneous emission to the optical mode, $k_{cav} = \omega/Q$ is the rate of loss of photons from the cavity (Q is the quality factor of the optical mode).

The rates of nonradiative processes are related to the rate of radiative transitions (k_r) and the internal quantum efficiency (Φ) in the following way: $\Phi = k_r/(k_r + k_{nr})$. The PL lifetime is, in turn, related to the rates of radiative and nonradiative transitions: $\tau_{PL} = 1/(k_r + k_{nr})$. Having estimated the quantum yield of luminescence of the material at 25% and determined lifetime $\tau_{PL} = 9.5$ ns by analyzing the experimental PL decay spectrum (Fig. 1, b), we obtain the following values: $1/k_r = 38$ ns and $1/k_{nr} = 12.6$ ns.

The parameters of the studied cavity structures needed to solve system (1a)–(1c) were determined using the transfer matrix method (absorption coefficient A) and the S -quantization method (Purcell factor F_p). The distributions of electric fields of modes localized in the active region (shown in Fig. 1, a) were used to calculate optical limiting factor $\Gamma = \int_0^d |E|^2 dx / \int_0^\infty |E|^2 dx$. Contribution β of spontaneous emission to modes was calculated as in [10] with the use of the experimental DPAVBi emission spectrum [7].

System (1a)–(1c) was solved numerically in the quasi-steady-state approximation ($dN_{exc}(t)/dt = 0$, $dN_{gr}(t)/dt = 0$, $dS(t)/dt = 0$) to determine the dependence of the output power, which is related to the photon density in the optical mode as $P = k_{cav} \hbar \omega SV / \Gamma$, on pumping power P_{pump} supplied to the structure. The parameters differing in two types of cavities and affecting the dependence of the output power are Γ , β , Q , F_p , and A . The calculation of these parameters yielded the following values for cavity type I: $\Gamma^I = 0.0824$, $\beta^I = 0.12$, $Q^I = 36.7$, $F_p^I = 9.38$, and $A^I = 0.73$; the corresponding values for cavity type II are $\Gamma^{II} = 0.0875$, $\beta^{II} = 0.07$,

$Q^{II} = 56.7$, $F_p^{II} = 12$, and $A^{II} = 0.7$. The calculation results are presented in Fig. 3. These values were used to determine threshold pumping powers ($P_{th}^I = 3.3$ W, $P_{th}^{II} = 3$ W) and differential efficiencies ($\eta^I = \frac{dP_{out}}{dP_{in}} = 0.613$, $\eta^{II} = \frac{dP_{out}}{dP_{in}} = 0.597$) for two types of cavities.

The considered structures feature close parameters of differential efficiency. Structure type II has lower threshold values, since its eigen mode has a higher quality factor (due to a higher reflection coefficient of the metallic mirror). The chosen structure parameters provide an opportunity to suppress the absorption of radiation in metallic elements. The combination of metallic and organic layers may allow one to balance efficient current pumping of the structure with the abstraction of heat from the active region.

Funding

This study was supported by the Russian Science Foundation (grant No. 21-12-00304).

Conflict of interest

The authors declare that they have no conflict of interest.

References

- [1] J.A. Lott, N.N. Ledentsov, V.M. Ustinov, N.A. Maleev, A.E. Zhukov, A.R. Kovsh, M.V. Maximov, B.V. Volovik, Zh.I. Alferov, D. Bimberg, *Electron. Lett.*, **36**, 1384 (2000). DOI: 10.1049/el:20000988
- [2] F. Koyama, *J. Lightwave Technol.*, **24**, 4502 (2006). DOI: 10.1109/JLT.2006.886064
- [3] S.A. Blokhin, M.A. Bobrov, A.G. Kuz'menkov, A.A. Blokhin, A.P. Vasil'ev, Yu.A. Guseva, M.M. Kulagina, Yu.M. Zadiranov, N.A. Maleev, I.I. Novikov, L.Ya. Karachinsky, N.N. Ledentsov, V.M. Ustinov, *Tech. Phys. Lett.*, **44** (1), 28 (2018). DOI: 10.1134/S1063785018010042.

- [4] M.A. Kaliteevski, A.A. Lazarenko, N.D. Il'inskaya, Yu.M. Zadiranov, M.E. Sasin, D. Zaitsev, V.A. Mazlin, P.N. Brunkov, S.I. Pavlov, A.Yu. Egorov, *Plasmonics*, **10**, 281 (2014). DOI: 10.1007/s11468-014-9806-0
- [5] G.M. Akselrod, E.R. Young, K.W. Stone, A. Palatnik, V. Bulović, Y.R. Tischler, *Phys. Rev. B*, **90**, 035209 (2014). DOI: 10.1103/PhysRevB.90.035209
- [6] R. Brückner, M. Sudzius, H. Fröb, V.G. Lyssenko, K. Leo, *J. Appl. Phys.*, **109**, 103116 (2011). DOI: 10.1063/1.3593188
- [7] K.M. Morozov, P. Pander, L.G. Franca, A.V. Belonovski, E.I. Girshova, K.A. Ivanov, D.A. Livshits, N.V. Selenin, G. Pozina, A.P. Monkman, M.A. Kaliteevski, *J. Phys. Chem. C*, **125**, 8376 (2021). DOI: 10.1021/acs.jpcc.1c02432
- [8] K.M. Morozov, E.I. Girshova, A.R. Gubaidullin, K.A. Ivanov, G. Pozina, M.A. Kaliteevski, *J. Phys.: Condens. Matter*, **30**, 435304 (2018). DOI: 10.1088/1361-648X/aae18c
- [9] M. Koschorreck, R. Gehlhaar, V.G. Lyssenko, M. Swoboda, M. Hoffmann, K. Leo, *Appl. Phys. Lett.*, **87**, 181108 (2005). DOI: 10.1063/1.2125128
- [10] G. van Soest, A. Lagendijk, *Phys. Rev. E*, **65**, 047601 (2002). DOI: 10.1103/PhysRevE.65.047601